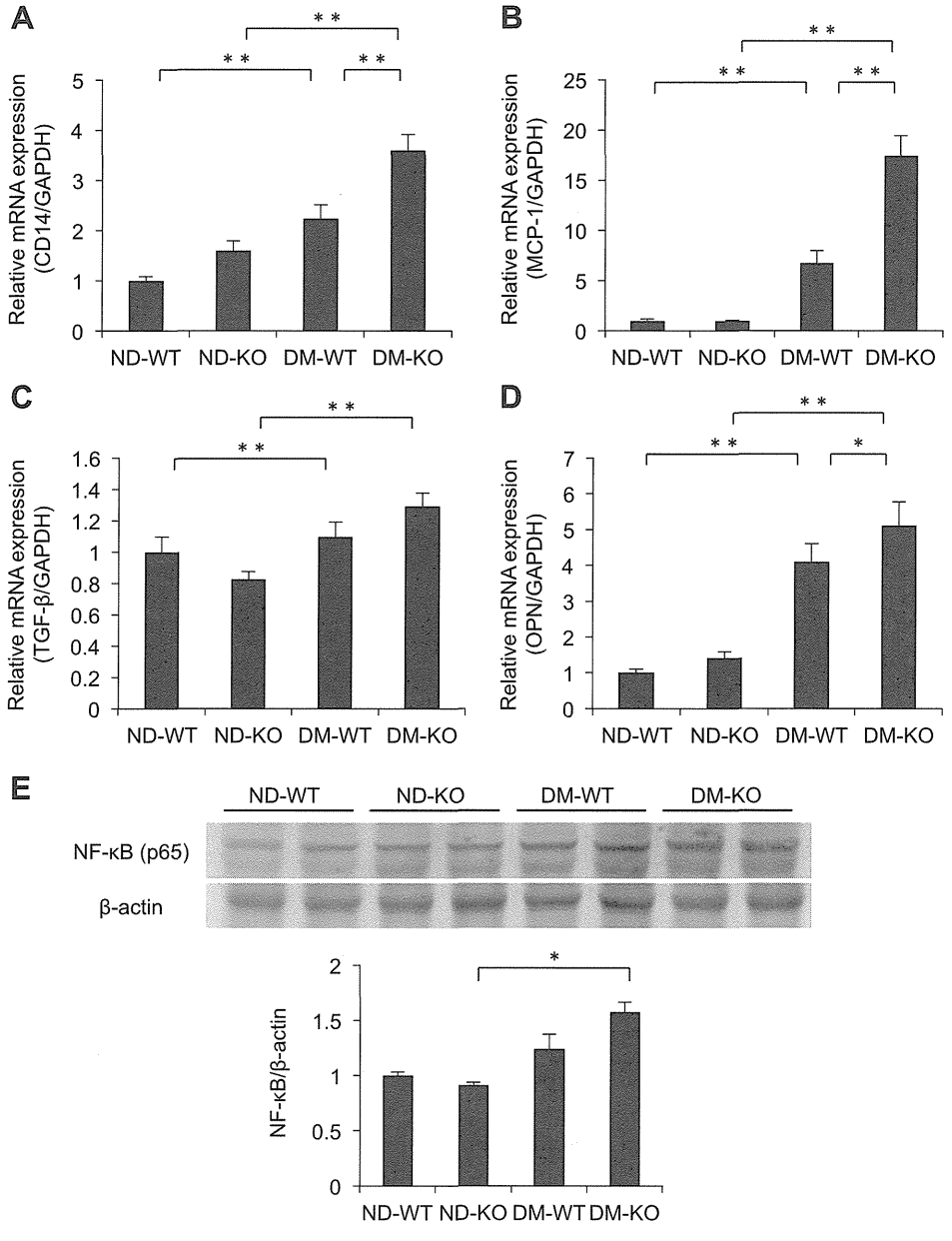

Fig. 4. MT deficiency accelerates diabetes-induced renal inflammation and macrophage infiltration. *A–D*: quantitative RT-PCR analysis of the expression levels of the macrophage marker CD14 and monocyte chemoattractant protein (MCP)-1 showed that MT deficiency promoted diabetes-induced macrophage infiltration into the kidney. Transforming growth factor (TGF)-β and osteopontin (OPN) mRNA levels were increased in the kidney in diabetic mice compared with nondiabetic mice, and were similar between DM-WT and DM-KO. mRNA levels were normalized to GAPDH. Values are means ± SE. $*P < 0.05$. $**P < 0.01$. *E*: Western blot analysis of NF-κB protein expression. NF-κB (p65) is significantly upregulated in DM-KO compared with ND-KO. Quantification was performed by densitometry of 3 independently performed experiments with normalization by β-actin. Values are means ± SE. $*P < 0.05$.

and to a lesser extent in the interstitium of nondiabetic $MT^{+/+}$ and $MT^{-/-}$ mice (Fig. 5*A*). Moreover, we assessed mitochondrial ROS production using MitoTracker Red CM-H_2XRos and MitoTracker Green FM staining. The intensity of MitoTracker Red CM-H_2XRos was higher in diabetic $MT^{-/-}$ mice compared with diabetic $MT^{+/+}$ mice (Fig. 5*B*). These findings suggest that MT deficiency increases diabetes-induced mitochondrial ROS in the interstitium of the kidney.

Mitochondrial morphology deteriorated in diabetic $MT^{-/-}$ mice. To confirm the beneficial effects of MT on generating mitochondrial ROS, we examined renal morphology in more detail using electron microscopy. The number of swollen mitochondria was increased, and cristae were also prominently reduced in renal proximal tubular cells of diabetic $MT^{+/+}$ mice compared with nondiabetic $MT^{+/+}$ mice, and were further increased in diabetic $MT^{-/-}$ mice compared with diabetic $MT^{+/+}$ mice (Fig. 6). These results indicate that MT deficiency impaired mitochondrial function in renal proximal tubular epithelial cells in the diabetic kidney.

ROS and inflammatory gene expression levels were increased by knockdown of MT in cultured proximal tubular epithelial cells. Mouse mProx24 renal proximal tubular epithelial cells were transfected with MT siRNA or scrambled siRNA as a control and subjected to qRT-PCR analyses and ELISA. MT mRNA and protein expression was significantly inhibited in MT knockdown cells compared with control cells (Fig. 7, *A* and *B*). High-glucose-induced Nox4 mRNA expression was increased in MT knockdown cells (Fig. 7*C*). To evaluate mitochondrial ROS in the mProx24 cells, we performed double staining using MitoTracker Red CM-H_2XRos and MitoTracker Green FM. The intensity of MitoTracker Red CM-H_2XRos was increased in mProx24 cells transfected with MT siRNA (Fig. 7*G*). Similarly, expression levels of inflammatory genes including MCP-1, TGF-β, and OPN were upregulated by MT RNAi (Fig.

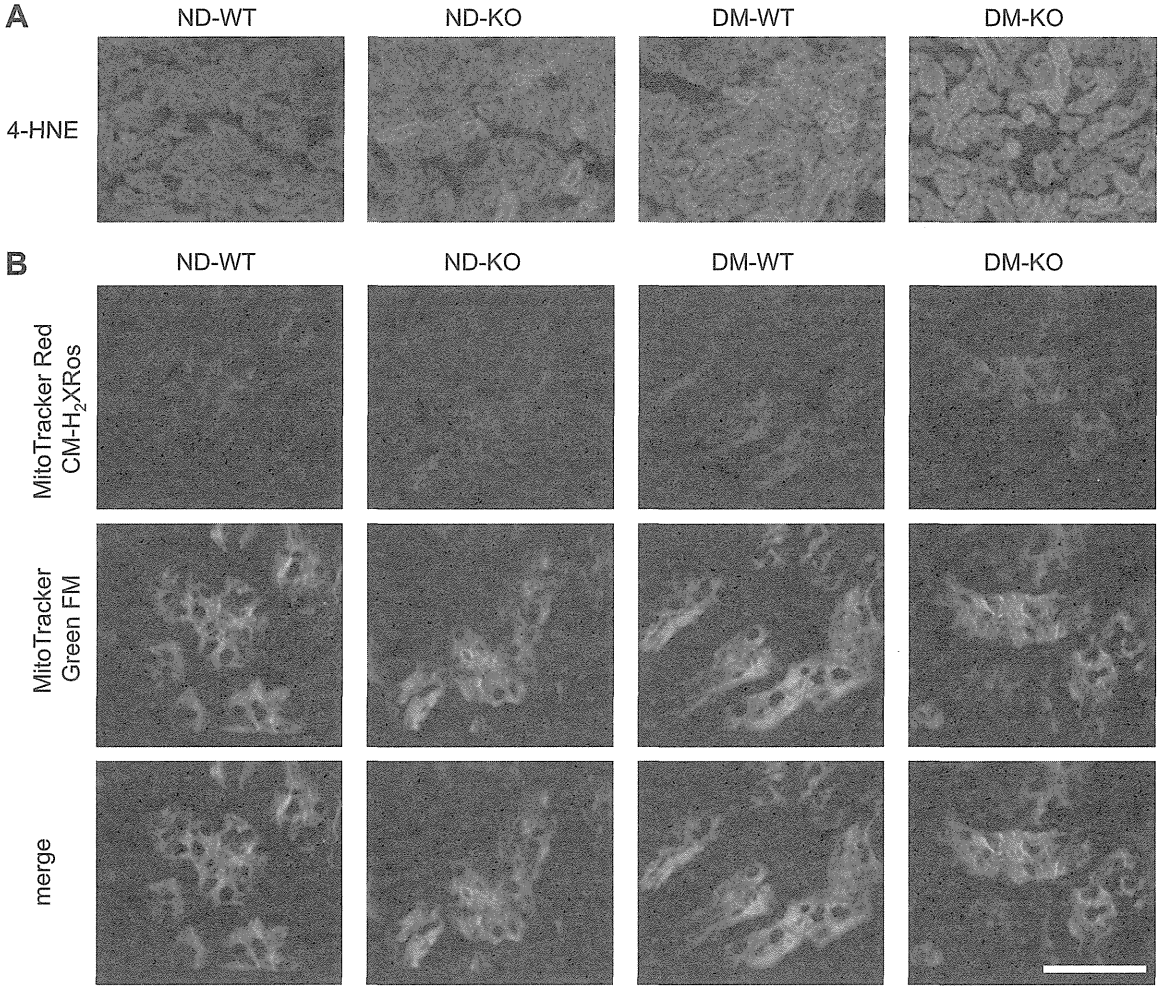

Fig. 5. MT deficiency induced accumulation of mitochondrial reactive oxygen species (ROS) in the diabetic kidney. *A*: oxidative stress was evaluated by fluorescence microscopy examinations using anti-4-hydroxynonenal (4-HNE) antibody. The intensity of 4-HNE was evident in DM-KO. Original magnification: ×100. *B*: mitochondrial ROS production was detected by fluorescence microscopy examinations using MitoTracker Red CM-H_2XRos and MitoTracker Green FM. The intensity of MitoTracker Red CM-H_2XRos was significantly increased in DM-KO compared with DM-WT. Original magnification: ×100.

7, *D–F*). These findings suggest that knockdown of MT exacerbates high-glucose-induced oxidative stress and inflammation in renal proximal tubular epithelial cells.

DISCUSSION

In the present study, we demonstrated that MT deficiency accelerated albuminuria and interstitial fibrosis without affecting blood glucose levels in STZ-induced diabetic mice. Macrophage infiltration in the interstitium of the diabetic kidney and the expression of inflammatory genes, including MCP-1, TGF-β, and OPN, were increased in diabetic $MT^{-/-}$ mice. Furthermore, mitochondrial ROS were increased and mitochondria were fragmented in diabetic $MT^{-/-}$ mice. In vitro studies with proximal tubular epithelial cells revealed that knockdown of MT increased the expression of Nox4, which was associated with oxidative stress, and expression of inflammatory genes. Our findings suggest that MT has antioxidative and anti-inflammatory effects in diabetic kidneys and prevents the development of diabetic nephropathy, independently of blood glucose levels.

MT comprise a family of low-molecular-weight, cysteine-rich, ubiquitous, and inducible intracellular proteins that bind to heavy metals such as zinc, copper, and cadmium and participate in metal homeostasis and detoxification (1). The mammalian MT family comprises four isoforms: MT-1, MT-2, MT-3, and MT-4. MT-3 is predominantly brain specific and is expressed in neurons and stimulated glial cells (16), while the two major isoforms, MT-1/-2, are expressed in most organs. However, the expression of MT in the kidney has been unclear. This and our recent study demonstrated that MT-1/-2 were highly induced in renal proximal tubular epithelial cells in diabetic mice (Fig. 3) and rats (21). This study also showed that MT has previously been reported to be a potent antioxidant; protecting cells from oxidative damage (2, 5, 9, 17, 18). We therefore hypothesized that MT may be induced in the kidney as an antioxidative protein and thus protect the kidney from diabetes-induced ROS and inflammation.

Many studies have proposed an important role of oxidative stress in the pathogenesis of diabetic nephropathy (3, 11, 29). We evaluated oxidative stress in the kidney by assessing mitochondrial ROS generation. MitoTracker Red CM-H_2XRos and MitoTracker Green FM staining revealed that mitochondrial ROS were increased in the interstitium, mainly in the tubular epithelial cells, of diabetic $MT^{-/-}$ mice compared with

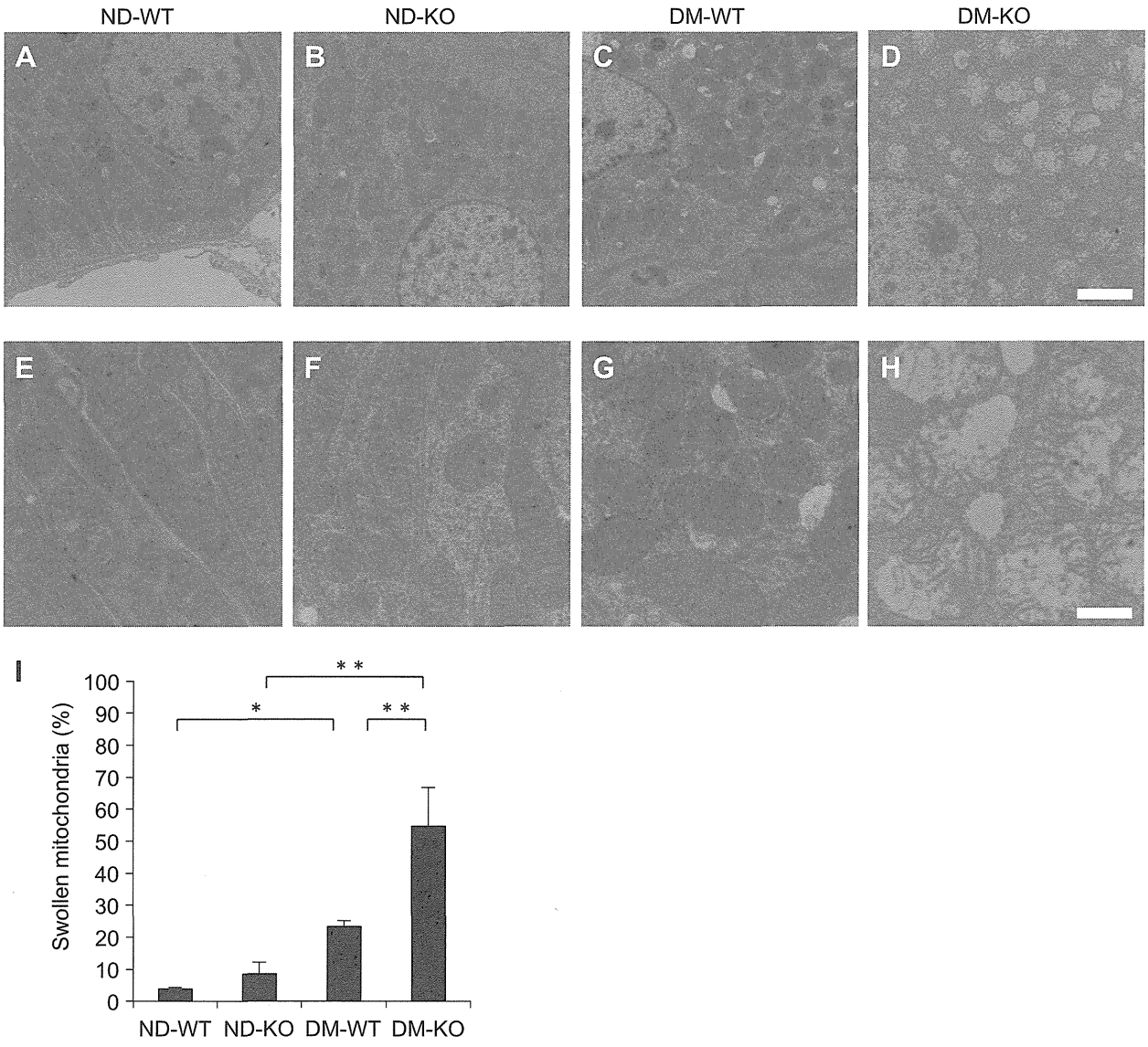

Fig. 6. Representative electron micrographs of proximal tubular epithelial cells in ND-WT (*A* and *E*), ND-KO (*B* and *F*), DM-WT (*E* and *G*), and DM-KO (*D* and *H*) mice. Original magnification: ×1,500 (*top*) and ×4,000 (*bottom*). Swollen mitochondria were increased in proximal tubular epithelial cells of DM-KO mice. Scale bar = 20 μm (*top*) and = 7.5 μm (*bottom*). *I*: quantitative analysis of swollen mitochondria. Swollen mitochondria were evident in diabetic mice and were significantly increased in DM-KO compared with DM-WT. Values are means ± SE. $*P < 0.05$. $**P < 0.01$.

diabetic $MT^{+/+}$ mice. Electron microscopy also showed more severe mitochondrial swelling in proximal tubular epithelial cells in diabetic $MT^{-/-}$ mice compared with diabetic $MT^{+/+}$ mice. It has been reported that mitochondrial morphology is altered in renal diseases including diabetic nephropathy (8, 31, 32). Since MT is a potent antioxidant and adaptive protein that protects cells and tissues from oxidative stress (12), we speculated that MT deficiency is likely to contribute to increased mitochondrial swelling in diabetic $MT^{-/-}$ mice. However, no studies have reported how MT is related to mitochondrial morphology, and thus further studies are needed. We also performed siRNA experiments to explore the effects of MT on the gene expression level of Nox4, as a promoter of ROS generation, and on the mitochondrial ROS in cultured proximal tubular epithelial cells. The fact that Nox4 expression and the intensity of MitoTracker Red CM-H_2XRos were increased by knockdown of MT suggests that MT may prevent Nox4-derived ROS generation by reducing oxidative stress in proximal tubular epithelial cells. Overall, these results indicate that MT deficiency increases diabetes-induced oxidative stress in the interstitium of the kidney.

Inflammation is also associated with the development of diabetic nephropathy (13, 15, 19). The present study revealed that increased expression levels of the macrophage marker CD14, the chemokine MCP-1, and the cytokines TGF-β and OPN noted in diabetic $MT^{+/+}$ mice were further increased in diabetic $MT^{-/-}$ mice. Similarly, macrophage infiltration into the interstitium and interstitial fibrosis were increased in diabetic $MT^{-/-}$ mice compared with diabetic $MT^{+/+}$ mice. However, macrophage infiltration in the glomeruli and mesangial matrix accumulation were similar in both types of mice. Moreover, in vitro studies demonstrated that the expression levels of inflammatory genes including MCP-1, TGF-β, and OPN were increased by knockdown of MT in cultured proxi-

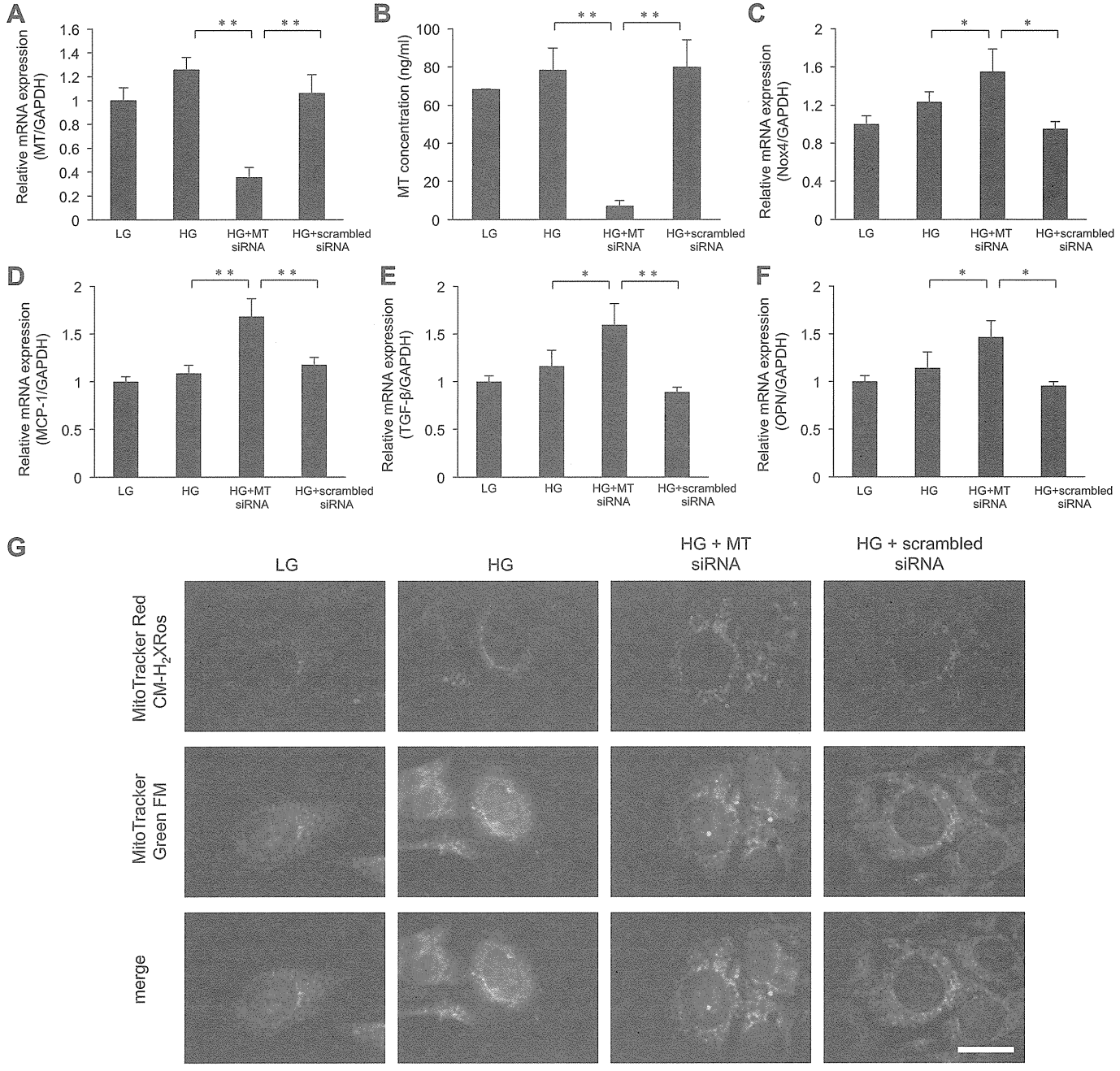

Fig. 7. MT knockdown accelerates high-glucose-induced oxidative stress and inflammation in cultured proximal tubular epithelial cells. *A* and *B*: MT mRNA and protein expression was significantly inhibited in mProx24 cells grown in high-glucose (HG) medium and transfected with MT small interfering (si) RNA compared with cells grown in HG medium and transfected with scrambled siRNA. HG, 25 mM; LG, low-glucose medium (5.5 mM). Values are means ± SE. $^{**}P < 0.01$. *C–F*: quantitative RT-PCR analysis showed that knockdown of MT increased the expression of NADPH oxidase 4 (Nox4) in proximal tubular epithelial cells. MCP-1, TGF-β, and OPN mRNA levels were also increased by MT siRNA, which indicated that knockdown of MT promoted inflammation in proximal tubular epithelial cells. mRNA levels are normalized to GAPDH. HG, 25 mM; LG, 5.5 mM. Values are means ± SE. $^{*}P < 0.05$. $^{**}P < 0.01$. *G*: representative photomicrographs of double immunofluorescent staining using MitoTracker Red CM-H_2XRos and MitoTracker Green FM. The intensity of MitoTracker Red CM-H_2XRos was increased in mProx24 cells transfected with MT siRNA compared with cells transfected with scrambled siRNA. HG, 25 mM; LG, 5.5 mM. Original magnification: ×200.

mal tubular epithelial cells. These results indicate that MT deficiency involves inflammation in the interstitium, but not in the glomeruli, in diabetic nephropathy. The expression of NF-κB, a master regulator of inflammatory genes, is increased in diabetic $MT^{-/-}$ mice compared with diabetic $MT^{+/+}$ mice. This result suggests that MT may suppress high-glucose-induced inflammation by inhibiting NF-κB.

We and others (14, 27) have demonstrated that MT plays a protective role in chronic kidney injury models induced by cadmium or cisplatin in the MT knockout mouse, but no studies have been reported in experimental models of diabetic nephropathy in the MT knockout mouse. Although we have previously shown that MT is upregulated in the kidney of the STZ-induced diabetic rat (21), whether MT prevents diabetes-

induced oxidative stress and inflammation, and thus protects against diabetic nephropathy, remains unclear. Podocyte-specific MT-transgenic mice showed that overexpression of MT in podocytes could ameliorate the primary features of diabetic nephropathy (33), suggesting that protection of the podocytes could inhibit diabetic nephropathy. Induction of renal tubular MT synthesis by zinc supplementation also prevents diabetic nephropathy by acting against oxidative stress (23, 28). Our current and previous study (21) showed that MT is induced mainly in renal tubules, rather than podocytes, in the diabetic kidney. Therefore, MT in renal proximal tubular epithelial cells might thus be a therapeutic target for the treatment of diabetic nephropathy.

In conclusion, we demonstrated that MT deficiency accelerates high-glucose-induced oxidative stress and inflammation in the kidney. The results of this study indicate that MT plays an important role in protecting the kidney from diabetic stress by acting as an antioxidant protein. Our findings suggest that MT might be a novel therapeutic target for the treatment of diabetic nephropathy.

GRANTS

This study was supported in part by a Grant-in-Aid for Scientific Research (C) to D. Ogawa (25461223) and a Grant-in-Aid for Young Scientists (B) to C. S. Horiguchi (24790927) from the Ministry of Education, Culture, Sports, Science, and Technology, and a Grant-in-Aid for Diabetic Nephropathy and Nephrosclerosis Research from the Ministry of Health, Labour, and Welfare of Japan. This work was also supported by the Naito Foundation and the Takeda Science Foundation.

DISCLOSURES

D. Ogawa and A. Nakatsuka belong to the Department of Diabetic Nephropathy, endowed by Astellas and Boehringer Ingelheim. J. W. is a consultant for Boehringer Ingelheim and receives speaker honoraria from Novartis. H. M. is a consultant for AbbVie and Astellas, receives speaker honoraria from Astellas, MSD, Takeda, and Tanabe Mitsubishi, and receives grant support from Astellas, Daiichi Sankyo, Dainippon Sumitomo, MSD, Novo Nordisk, and Takeda. The authors report no conflicts of interest in this work.

AUTHOR CONTRIBUTIONS

Author contributions: H.T., N.S., M.A., I.M., N.T., T.H., C.S.H., A.N., and H.Y. performed experiments; H.T. and J.E. analyzed data; H.T., D.O., N.S., M.A., I.M., N.T., T.H., C.S.H., A.N., and J.E. interpreted results of experiments; H.T., J.W., and H.Y. prepared figures; H.T. and D.O. drafted manuscript; H.T., D.O., N.S., M.A., I.M., N.T., T.H., C.S.H., A.N., J.E., J.W., H.Y., K.T., and H.M. approved final version of manuscript; D.O. conception and design of research; J.W., H.Y., K.T., and H.M. edited and revised manuscript.

REFERENCES

1. **Aschner M.** Metallothionein (MT) isoforms in the central nervous system (CNS): regional and cell-specific distribution and potential functions as an antioxidant. *Neurotoxicology* 19: 653–660, 1998.
2. **Cai L, Klein JB, Kang YJ.** Metallothionein inhibits peroxynitrite-induced DNA and lipoprotein damage. *J Biol Chem* 275: 38957–38960, 2000.
3. **Dong YF, Liu L, Kataoka K, Nakamura T, Fukuda M, Tokutomi Y, Nako H, Ogawa H, Kim-Mitsuyama S.** Aliskiren prevents cardiovascular complications and pancreatic injury in a mouse model of obesity and type 2 diabetes. *Diabetologia* 53: 180–191, 2010.
4. **Dronavalli S, Duka I, Bakris GL.** The pathogenesis of diabetic nephropathy. *Nat Clin Pract Endocrinol Metab* 4: 444–452, 2008.
5. **Ebadi M, Brown-Borg H, El Refaey H, Singh BB, Garrett S, Shavali S, Sharma SK.** Metallothionein-mediated neuroprotection in genetically engineered mouse models of Parkinson's disease. *Brain Res Mol Brain Res* 134: 67–75, 2005.
6. **Forbes JM, Coughlan MT, Cooper ME.** Oxidative stress as a major culprit in kidney disease in diabetes. *Diabetes* 57: 1446–1454, 2008.
7. **Giacco F, Brownlee M.** Oxidative stress and diabetic complications. *Circ Res* 107: 1058–1070, 2010.
8. **Kaneda K, Iwao J, Sakata N, Takebayashi S.** Correlation between mitochondrial enlargement in renal proximal tubules and microalbuminuria in rats with early streptozotocin-induced diabetes. *Acta Pathol Jpn* 42: 855–860, 1992.
9. **Kang YJ, Chen Y, Yu A, Voss-McCowan M, Epstein PN.** Overexpression of metallothionein in the heart of transgenic mice suppresses doxorubicin cardiotoxicity. *J Clin Invest* 100: 1501–1506, 1997.
10. **Kanwar YS, Sun L, Xie P, Liu FY, Chen S.** A glimpse of various pathogenetic mechanisms of diabetic nephropathy. *Annu Rev Pathol* 6: 395–423, 2011.
11. **Kodera R, Shikata K, Kataoka HU, Takatsuka T, Miyamoto S, Sasaki M, Kajitani N, Nishishita S, Sarai K, Hirota D, Sato C, Ogawa D, Makino H.** Glucagon-like peptide-1 receptor agonist ameliorates renal injury through its anti-inflammatory action without lowering blood glucose level in a rat model of type 1 diabetes. *Diabetologia* 54: 965–978, 2011.
12. **Li X, Cai L, Feng W.** Diabetes and metallothionein. *Mini Rev Med Chem* 7: 761–768, 2007.
13. **Lin M, Yiu WH, Wu HJ, Chan LY, Leung JC, Au WS, Chan KW, Lai KN, Tang SC.** Toll-like receptor 4 promotes tubular inflammation in diabetic nephropathy. *J Am Soc Nephrol* 23: 86–102, 2012.
14. **Liu Y, Liu J, Habeebu SM, Waalkes MP, Klaassen CD.** Metallothionein-I/II null mice are sensitive to chronic oral cadmium-induced nephrotoxicity. *Toxicol Sci* 57: 167–176, 2000.
15. **Matsushita Y, Ogawa D, Wada J, Yamamoto N, Shikata K, Sato C, Tachibana H, Toyota N, Makino H.** Activation of peroxisome proliferator-activated receptor delta inhibits streptozotocin-induced diabetic nephropathy through anti-inflammatory mechanisms in mice. *Diabetes* 60: 960–968, 2011.
16. **Miyazaki I, Asanuma M, Higashi Y, Sogawa CA, Tanaka K, Ogawa N.** Age-related changes in expression of metallothionein-III in rat brain. *Neurosci Res* 43: 323–333, 2002.
17. **Miyazaki I, Asanuma M, Hozumi H, Miyoshi K, Sogawa N.** Protective effects of metallothionein against dopamine quinone-induced dopaminergic neurotoxicity. *FEBS Lett* 581: 5003–5008, 2007.
18. **Miyazaki I, Asanuma M, Kikkawa Y, Takeshima M, Murakami S, Miyoshi K, Sogawa N, Kita T.** Astrocyte-derived metallothionein protects dopaminergic neurons from dopamine quinone toxicity. *Glia* 59: 435–451, 2011.
19. **Nagase R, Kajitani N, Shikata K, Ogawa D, Kodera R, Okada S, Kido Y, Makino H.** Phenotypic change of macrophages in the progression of diabetic nephropathy; sialoadhesin-positive activated macrophages are increased in diabetic kidney. *Clin Exp Nephrol* 16: 739–748, 2012.
20. **Navarro-Gonzalez JF, Mora-Fernandez C, Muros de Fuentes M, Garcia-Perez J.** Inflammatory molecules and pathways in the pathogenesis of diabetic nephropathy. *Nat Rev Nephrol* 7: 327–340, 2011.
21. **Ogawa D, Asanuma M, Miyazaki I, Tachibana H, Wada J, Sogawa N, Sugaya T, Kitamura S, Maeshima Y, Shikata K, Makino H.** High glucose increases metallothionein expression in renal proximal tubular epithelial cells. *Exp Diabetes Res* 2011: 534872, 2011.
22. **Okada S, Shikata K, Matsuda M, Ogawa D, Usui H, Kido Y, Nagase R, Wada J, Shikata Y, Makino H.** Intercellular adhesion molecule-1-deficient mice are resistant against renal injury after induction of diabetes. *Diabetes* 52: 2586–2593, 2003.
23. **Ozcelik D, Naziroglu M, Tuncdemir M, Celik O, Ozturk M, Flores-Arce MF.** Zinc supplementation attenuates metallothionein and oxidative stress changes in kidney of streptozotocin-induced diabetic rats. *Biol Trace Elem Res* 150: 342–349, 2012.
24. **Palmiter RD.** The elusive function of metallothioneins. *Proc Natl Acad Sci USA* 95: 8428–8430, 1998.
25. **Sarnak MJ, Levey AS, Schoolwerth AC, Coresh J, Culleton B, Hamm LL, McCullough PA, Kasiske BL, Kelepouris E, Klag MJ, Parfrey P, Pfeffer M, Raij L, Spinosa DJ, Wilson PW.** Kidney disease as a risk factor for development of cardiovascular disease: a statement from the American Heart Association Councils on Kidney in Cardiovascular Disease, High Blood Pressure Research, Clinical Cardiology, and Epidemiology and Prevention. *Circulation* 108: 2154–2169, 2003.
26. **Shikata K, Makino H.** Role of macrophages in the pathogenesis of diabetic nephropathy. *Contrib Nephrol* 46–54, 2001.
27. **Sogawa N, Hirai K, Sogawa C, Ohyama K, Miyazaki I, Tsukamoto G, Asanuma M, Sasaki A, Kitayama S.** Protective effect of cepharanthin on

cisplatin-induced renal toxicity through metallothionein expression. *Life Sci* 92: 727–732, 2013.
28. **Tang Y, Yang Q, Lu J, Zhang X, Suen D, Tan Y, Jin L, Xiao J, Xie R, Rane M, Li X, Cai L.** Zinc supplementation partially prevents renal pathological changes in diabetic rats. *J Nutr Biochem* 21: 237–246, 2010.
29. **Toyonaga J, Tsuruya K, Ikeda H, Noguchi H, Yotsueda H, Fujisaki K, Hirakawa M, Taniguchi M, Masutani K, Iida M.** Spironolactone inhibits hyperglycemia-induced podocyte injury by attenuating ROS production. *Nephrol Dial Transplant* 26: 2475–2484, 2011.
30. **Vasak M.** Advances in metallothionein structure and functions. *J Trace Elem Med Biol* 19: 13–17, 2005.
31. **Wang W, Wang Y, Long J, Wang J, Haudek SB, Overbeek P, Chang BH, Schumacker PT, Danesh FR.** Mitochondrial fission triggered by hyperglycemia is mediated by ROCK1 activation in podocytes and endothelial cells. *Cell Metab* 15: 186–200, 2012.
32. **Zhan M, Brooks C, Liu F, Sun L, Dong Z.** Mitochondrial dynamics: regulatory mechanisms and emerging role in renal pathophysiology. *Kidney Int* 83: 568–581, 2013.
33. **Zheng S, Carlson EC, Yang L, Kralik PM, Huang Y, Epstein PN.** Podocyte-specific overexpression of the antioxidant metallothionein reduces diabetic nephropathy. *J Am Soc Nephrol* 19: 2077–2085, 2008.

Predictive Properties of Plasma Amino Acid Profile for Cardiovascular Disease in Patients with Type 2 Diabetes

Shinji Kume[1]*, Shin-ichi Araki[1], Nobukazu Ono[2], Atsuko Shinhara[2], Takahiko Muramatsu[2], Hisazumi Araki[1], Keiji Isshiki[1], Kazuki Nakamura[2], Hiroshi Miyano[2], Daisuke Koya[3], Masakazu Haneda[4], Satoshi Ugi[1], Hiromichi Kawai[1], Atsunori Kashiwagi[1], Takashi Uzu[1], Hiroshi Maegawa[1]

1 Department of Medicine, Shiga University of Medical Science, Otsu, Shiga, Japan, **2** Institute for Innovation, Ajinomoto Co., Inc., Kawasaki, Kanagawa, Japan, **3** Division of Diabetology & Endocrinology, Kanazawa Medical University, Kahoku-Gun, Ishikawa, Japan, **4** Division of Metabolism and Biosystemic Science, Department of Medicine, Asahikawa Medical University, Asahikawa, Hokkaido, Japan

Abstract

Prevention of cardiovascular disease (CVD) is an important therapeutic object of diabetes care. This study assessed whether an index based on plasma free amino acid (PFAA) profiles could predict the onset of CVD in diabetic patients. The baseline concentrations of 31 PFAAs were measured with high-performance liquid chromatography-electrospray ionization-mass spectrometry in 385 Japanese patients with type 2 diabetes registered in 2001 for our prospective observational follow-up study. During 10 years of follow-up, 63 patients developed cardiovascular composite endpoints (myocardial infarction, angina pectoris, worsening of heart failure and stroke). Using the PFAA profiles and clinical information, an index (CVD-AI) consisting of six amino acids to predict the onset of any endpoints was retrospectively constructed. CVD-AI levels were significantly higher in patients who did than did not develop CVD. The area under the receiver-operator characteristic curve of CVD-AI (0.72 [95% confidence interval (CI): 0.64–0.79]) showed equal or slightly better discriminatory capacity than urinary albumin excretion rate (0.69 [95% CI: 0.62–0.77]) on predicting endpoints. A multivariate Cox proportional hazards regression analysis showed that the high level of CVD-AI was identified as an independent risk factor for CVD (adjusted hazard ratio: 2.86 [95% CI: 1.57–5.19]). This predictive effect of CVD-AI was observed even in patients with normoalbuminuria, as well as those with albuminuria. In conclusion, these results suggest that CVD-AI based on PFAA profiles is useful for identifying diabetic patients at risk for CVD regardless of the degree of albuminuria, or for improving the discriminative capability by combining it with albuminuria.

Citation: Kume S, Araki S-i, Ono N, Shinhara A, Muramatsu T, et al. (2014) Predictive Properties of Plasma Amino Acid Profile for Cardiovascular Disease in Patients with Type 2 Diabetes. PLOS ONE 9(6): e101219. doi:10.1371/journal.pone.0101219

Editor: Matej Oresic, Steno Diabetes Center, Denmark

Received January 15, 2014; **Accepted** June 4, 2014; **Published** June 27, 2014

Funding: This study was partly funded by Ajinomoto Co., Inc. Some of authors, NO, AS, TM, KN, and H. Miyano, are employees of Ajinomoto, Co., Inc. They contributed to the design of study, analysis of the data and describing the manuscript. However, this does not alter the authors' adherence to all the journal policies on sharing data and materials. This study was also granted by the Grants-in-Aid for Scientific Research (KAKENHI) from Japan Society for the Promotion of Science (No. 25713033 to S.K. and No. 70242980 to DK) and a Grant-in-Aid for Diabetic Nephropathy and Nephrosclerosis Research from Ministry of Health, Labour and Welfare of Japan (SA). The funders had no role in study design, data collection and analysis, decision to publish, or preparation of the manuscript.

Competing Interests: NO, AS, TM, KN, and H. Miyano are employees of Ajinomoto, Co., Inc. This does not alter the authors' adherence to all the journal policies on sharing data and materials.

* Email: skume@belle.shiga-med.ac.jp

Introduction

Cardiovascular disease (CVD) is a life-threatening complication in patients with diabetes. Since hyperglycemia, hypertension, and dyslipidemia are well recognized as conventional risk factors for CVD, early intervention against them is important to prevent the onset of CVD in this population [1]. Several clinical studies have indicated that the incidence of CVD in patients with type 2 diabetes could be reduced with intensive management for these risk factors [2,3]. The development of biomarkers or an index to identify patients at high risk for CVD is also clinically important as it makes possible the initiation of adequate medication for patients at risk. Excessive urinary albumin excretion, called albuminuria, has been established as a reliable surrogate biomarker for CVD, because an increase or decrease in albuminuria has been reported to directly affect the incidence of CVD [3–5]. Thus, the prevention and reduction of albuminuria by intensive control of the above-mentioned conventional risk factors for CVD is considered an important therapeutic target in the care of patients with diabetes [2,6,7]. Despite these efforts, however, many patients still develop CVD, suggesting that only the evaluation of known risk factors is insufficient to distinguish between patients at high and low risk of CVD. It is therefore important that an additional predictive biomarker or index be found to identify those patients with diabetes who are at risk for CVD.

Recent studies have reported that alteration of plasma metabolomics profiles is significantly associated with certain disease conditions and can predict future development of diseases [8–11]. Among the numerous metabolites, plasma free amino acids (PFAAs) may be potent metabolites that have potential as excellent disease biomarkers because circulating free amino acids are involved in protein synthesis, organ networks, and as metabolic regulators of physiological states [12]. Recent technological advances have made possible the highly accurate analysis of PFAA levels using high-performance liquid chromatography-electrospray ionization-mass spectrometry (HPLC-ESI-MS) [13].

We have previously reported on the possibility of this technical approach being able to distinguish patients with lung cancer [14].

In the current study, we hypothesized that alterations in PFAA profiles may be early markers for identifying diabetic patients at risk for CVD. We measured PFAA profiles in plasma samples of patients with type 2 diabetes enrolled in our ongoing prospective observational follow-up study. We retrospectively investigated whether we could construct a diagnostic index based on these PFAA profiles, known as "AminoIndex^{TM} (AI) technology" [12–14], and whether this index could predict the onset of CVD in patients with type 2 diabetes followed up for 10 years.

Materials and Methods

Ethics statement

The study protocol and informed consent procedure were approved by the Ethics Committee of Shiga University of Medical Science (Shiga, Japan) and Ajinomoto Co., Inc. (Kawasaki, Japan). This study was conducted according to the principles expressed in the Declaration of Helsinki. The raw data used in this study have not been deposited in a public database. This is in compliance with the agreement with the Ethics Committee.

Subjects

This study was a retrospective analysis of samples obtained during our ongoing prospective observational study, the Shiga Prospective Observational Follow-up Study [15]. This prospective follow-up study was launched in 1996 to assess patient characteristics associated with the development and progression of diabetic complications, and to identify biomarkers and genetic factors that can be used in the early detection of diabetic patients at risk for these complications.

Diabetic patients who agreed to participate in this study and provided written informed consent were asked to provide a 24-h urine sample at baseline. Baseline blood samples were obtained after an overnight fast in tubes containing ethylenediaminetetraacetic acid. Plasma was prepared by centrifuging the blood samples at 3,000 rpm at 4°C for 15 min. If not analyzed immediately, plasma and urine samples were stored at −80°C. All participants underwent annual standardized clinical examinations and biochemical tests. Each patient's medical records were reviewed annually and the occurrence of CVD, cancer, and other diseases was confirmed.

To assess whether an amino acid-based index could better predict the onset of CVD (CVD-AI) over 10 years than albuminuria and other conventional risk factors, we analyzed samples from 420 Japanese patients with type 2 diabetes registered in this prospective trial in 2001. The PFAAs in the stored plasma samples of each eligible patient were measured. Six patients were excluded from the study because their PFAAs could not be accurately measured, and seven patients were excluded because their urine samples were not available. In addition, 22 patients with a previous history at baseline of cancer, collagen disease, CVD within the previous year, infectious disease, or non-diabetic kidney disease confirmed by a renal biopsy were excluded. Thus, the data from 385 patients were finally analyzed in this study.

Definition of cardiovascular composite endpoints and clinical parameters

Cardiovascular composite endpoints were myocardial infarction, angina pectoris, worsening of congestive heart failure, and

Table 1. Baseline characteristics of patients who did (cases) and did not (controls) experience cardiovascular events during follow-up.

Variables	Controls	Cases	*P* value
Number (n)	322	63	
Age (year)	60±12	68±7	<0.01
Gender (male/female, n)	156/166	35/28	0.30
Body mass index (kg/m^2)	23.5±3.9	24.4±4.1	0.10
Hemoglobin A1c (%)	7.6±0.9	7.7±1.0	0.11
Total cholesterol (mg/dL)	206±30	207±29	0.70
Triglyceride (mg/dL)	92 (64–134)	104 (73–140)	0.14
HDL-cholesterol (mg/dL)	54 (46–65)	47 (41–55)	<0.01
Systolic blood pressure (mmHg)	135±19	143±20	<0.01
Diastolic blood pressure (mmHg)	76±11	75±10	0.49
Hypertension (%)	53.4	84.1	<0.01
Estimated GFR (ml/min/1.73m^2)	82±23	67±21	<0.01
Urinary albumin excretion rate (μg/min)	8.4 (5.1–24.8)	27.4 (8.3–113.2)	<0.01
Albuminuria (%)	26.4	55.6	<0.01
baPWV (m/sec)	1786±522	1974±567	<0.01
Myocardial infarction (n)	-	11	-
Angina pectoris (n)	-	29	-
Congestive heart failure (n)	-	5	-
Stroke (n)	-	18	-

Data are expressed as mean ± SD for normally distributed continuous variables or median (interquartile range) for skewed continuous variables.
Abbreviations: GFR, glomerular filtration rate; HDL, high density lipoprotein; baPWV, brachial-ankle pulse wave velocity.
doi:10.1371/journal.pone.0101219.t001

Table 2. Absolute levels of 31 plasma amino acids in patients who did (cases) and did not (controls) experience cardiovascular events during follow-up.

Amino Acids (μmol/l)	HMDB ID	Control (n = 328)	Case (n = 63)	*P* value
3-methylhistidine (3MeHis)	HMDB01861	2.3±1.6	3.5±2.8	0.001
Citrulline (Cit)	HMDB00904	38.0±13.2	43.1±15.1	0.016
Tryptophan (Trp)	HMDB00929	60.5±13.0	55.3±13.0	0.016
β-amino-iso-butyric acid (β-AIBA)	Not available	1.6±2.0	2.2±2.3	0.033
Cystine (Cys)	HMDB00192	55.8±13.7	60.0±15.5	0.048
Glutamic acid (Glu)	HMDB00148	33.2±14.7	37.1±16.2	0.078
α-amino adipic acid (α-AAA)	HMDB00510	0.3±0.6	0.4±0.7	0.105
Threonine (Thr)	HMDB00167	130.0±31.2	122.2±32.2	0.118
Methionine (Met)	HMDB00696	27.5±5.8	26.5±5.7	0.153
Serine (Ser)	HMDB00187	116.8±22.5	112.3±21.3	0.160
Histidine (His)	HMDB00177	81.3±11.8	79.1±10.8	0.205
Ethanolamine (EtOHNH2)	HMDB00149	6.9±1.6	6.6±1.5	0.242
Prorine (Pro)	HMDB00162	150.6±41.0	157.3±42.6	0.298
Taurine (Tau)	HMDB00251	61.4±15.1	62.3±13.0	0.307
Arginine (Arg)	HMDB00517	102.4±24.4	105.9±25.9	0.374
Hydroxyproline (HyPro)	HMDB00725	12.3±6.2	12.9±6.2	0.385
Aspartic acid (Asp)	HMDB00191	2.3±1.1	2.4±1.0	0.401
Asparagine (Asn)	HMDB00168	51.8±10.	51.0±10.	0.402
Phenylalanine (Phe)	HMDB00159	67.2±11.1	66.8±12.6	0.519
Ornithine (Orn)	HMDB00214	65.7±16.2	69.2±21.3	0.564
Tyrosine (Tyr)	HMDB00158	78.3±19.2	76.2±18.4	0.599
α-amino-n-butyric acid (α-ABA)	Not available	22.4±6.7	22.1±7.5	0.722
Valine (Val)	HMDB00883	250.3±45.8	245.5±43.5	0.741
Isoleucine (Ile)	HMDB00172	75.9±17.1	75.8±15.9	0.838
Glycine (Gly)	HMDB00123	227.2±54.9	228.5±53.8	0.851
Sarcosine (Sar)	HMDB00271	2.1±1.0	2.1±1.1	0.876
Glutamine (Gln)	HMDB00641	622.7±120.4	631.4±154.8	0.876
Leucine (Leu)	HMDB00687	137.0±27.2	135.2±26.3	0.926
1-methylhistidine (1MeHis)	HMDB00001	4.2±5.4	4.5±6.2	0.953
Alanine (Ala)	HMDB00161	428.7±94.6	427.5±93.1	0.954
Lysine (Lys)	HMDB00182	197.9±37.1	200.0±43.1	0.974

Abbreviations: HMDB ID: Human Metabolome Database ID.

doi:10.1371/journal.pone.0101219.t002

stroke [15]. Myocardial infarction was defined as a clinical presentation characterized by typical symptoms, electrocardiographic changes associated with an elevation of cardiac biomarkers, and angiographic evidence of coronary thrombosis. Angina pectoris was defined as the presence on imaging of lesions in patients with a history of typical chest pain or electrocardiographic changes, and invasive cardiovascular interventions. A worsening of congestive heart failure was defined as events requiring hospitalization for worsening typical symptoms of heart failure validated by echocardiography, not due to valvular heart disease or arrhythmia. Stroke, including ischemic stroke and cerebral hemorrhage, was defined as a persistent focal neurological symptom in which the onset was sudden and was not due to trauma or a tumor, and where the responsible lesion was detected on imaging modalities. If a patient died, his/her medical records were checked to identify the cause of death. If the cause of death was not clear, it was not considered related to CVD.

Based on the urinary albumin excretion rate (UAER) at baseline, patients were classified as having normoalbuminuria (UAER <20 μg/min, n = 265) or albuminuria (20 μg/min $\leq$ UAER, n = 120). Serum levels of creatinine were measured via an enzymatic method. Estimated glomerular filtration rate (eGFR) was calculated using the simplified equation proposed by the Japanese Society of Nephrology [16]: eGFR (ml/min/1.73 m^2) $= 194\times$ [age (years)]$^{-0.287}\times$ [serum creatinine (mg/dl)]$^{-1.094}$ $\times 0.739$ (for female patients). Hemoglobin A_{1c} (HbA1c) levels were those of the National Glycohemoglobin Standardization Program, according to the recommendations of the Japanese Diabetes Society [17]. Hypertension was defined as blood pressure (BP) $\geq$ 140/90 mmHg or current use of antihypertensive drugs. Brachial-ankle pulse wave velocity (baPWV) was measured by an automatic device (BP-203RPE; Colin, Komaki, Japan), with the higher of the right and the left values used in calculations.

PFAAs and CVD-AI

Plasma samples were deproteinized using acetonitrile at a final concentration of 80%, and amino acid levels in plasma were measured by HPLC-ESI-MS/MS, followed by precolumn derivatization, as described [13,14]. The concentrations of 31 amino acids were measured at the Institute for Innovation of the Ajinomoto Co., Inc. (Kawasaki, Japan).

Although the levels of PFAAs may differ significantly between cases and controls, the differences in individual amino acids are not always sufficiently discriminatory [14]. We therefore constructed a diagnostic index based on PFAA levels, known as "AminoIndex ^{TM} technology" [12–14], to compress multidimensional information from PFAA profiles into a single dimension and to maximize the differences between cases and controls. The CVD-AI index was defined as the logarithmic odds ratio of CVD probability estimated by logistic regression models. Briefly, we generated all possible models with six or fewer variables. During this step, all possible combinations of variables were considered from a total of 31 amino acids [14]. Next, we calculated the area under the curve (AUC) for receiver-operator characteristic (ROC) curve analysis for all models with non-validation or leave-one-out cross validation (LOOCV). The model which produced the highest AUC for ROC curve analysis by LOOCV was selected as the final model, CDV-AI. Table S1 explains the top 10 models' performances using the AUC for ROC curve analysis.

Statistical analysis

Clinical data are expressed as mean ± SD or median (interquartile range), as appropriate. Categorical variables were compared using χ^2 tests, normally distributed continuous variables using unpaired Student's *t*-tests, and abnormally distributed continuous variables using the Mann–Whitney U test. In particular, differences in amino acid levels and the CVD-AI between the two groups were assessed by the Mann–Whitney U test. Spearman's rank correlation coefficient (ρ) was used to assess the correlation between each amino acid level and clinical variables. ROC curve analysis was performed to determine the capability and cut-off level of variables that distinguished between cases and controls. The 95% confidence interval (CI) of the AUC for ROC was also estimated. The unadjusted (crude) and adjusted hazard ratios (HR) for the occurrence of cardiovascular events were evaluated using a Cox proportional hazards regression model. Follow-up time was censored if any cardiovascular composite endpoint occurred or if the patient was unavailable for follow-up. To assess the risk factors for the cardiovascular composite endpoint, each variable listed in Table 1 and the CVD-AI were first evaluated using univariate analysis of the Cox proportional hazards regression model and then each estimate was adjusted for all variables showing statistical significance in the univariate model. To assess the combination effect of the CVD-AI and albuminuria, estimates were adjusted for the conventional risk factors of cardiovascular disease, including age, sex, HbA1c, total cholesterol, triglyceride, high density lipoprotein (HDL)-cholesterol, eGFR, body mass index (BMI) and hypertension. All analyses were performed using the SPSS software package (version 22; SPSS Inc., Chicago, IL, USA), with a two-sided *P* value of <0.05 considered statistically significant.

Results

Characteristics of subjects

During the 10-year follow-up period, 63 patients experienced cardiovascular endpoints, including 11 with myocardial infarction, 29 with angina pectoris, five with worsening of congestive heart failure, and 18 with stroke (Table 1). The clinical characteristics at baseline of these 63 patients with outcomes (cases) and the 322 without outcomes (controls) are presented in Table 1. Age, HDL-cholesterol, systolic BP, eGFR, UAER, and baPWV differed significantly in these two groups.

PFAA profiles related to cardiovascular composite endpoints

The mean levels of each amino acid in the case and control groups are shown in Table 2. Among the 31 amino acids tested, three (β-amino-iso-butyric acid, 3-methylhistidine, and citrulline) were significantly higher and one (tryptophan) was significantly lower in cases than in controls. Some amino acid levels showed statistically significant correlations with some clinical variables related to risk factors of cardiovascular disease (Table S2).

Predictive effect of CVD-AI

We next assessed whether the onset of the cardiovascular composite endpoint could be distinguished by the multivariate analysis referred to as AI technology. Using this technology, the optimal CVD-AI was constructed from the data set of PFAAs: CVD-AI = (−0.1452) + (−0.2230) × (ethanolamine) + (−0.04637) × (hydroxyproline) + (0.01303) × (glutamic acid) + (0.3524) × (3-methylhistidine) + (0.01250) × (tyrosine) + (−0.03093) × (tryptophan).

The mean value of the CVD-AI was significantly higher in cases than in controls (−1.28±0.94 *vs.* −1.90±0.69, $P<0.001$). The CVD-AI value was positively correlated with age ($\rho = 0.23$, $P< 0.01$), BMI ($\rho = 0.15$, $P<0.01$), triglyceride ($\rho = 0.18$, $P<0.01$), systolic BP ($\rho = 0.18$, $P<0.01$), baPWV ($\rho = 0.22$, $P<0.001$) and

Table 3. Areas under the receiver-operating characteristic curves distinguishing patients who did (cases) and did not (controls) experience cardiovascular events during follow-up.

Parameters	AUC (± SE)	(95% CI)	*P* value
β-AIBA (μmol/l)	0.59±0.04	(0.50–0.66)	0.002
3MeHis (μmol/l)	0.62±0.04	(0.55–0.71)	0.04
Cit (μmol/l)	0.59±0.04	(0.52–0.07)	0.04
Trp (μmol/l)	0.59±0.04	(0.52–0.67)	0.02
CVD-AI	0.72±0.04	(0.64–0.79)	<0.0001
UAER	0.69±0.04	(0.62–0.77)	<0.0001

Abbreviations: AUC, area under the receiver-operator characteristic curve; β-AIBA, β-amino-iso-butyric acid; 3MeHis, 3-methylhistidine; Cit, citrulline; Trp, tryptophan; Cys, cystine; CVD-AI, cardiovascular disease-amino acid based index; UAER, urinary albumin excretion rate.

doi:10.1371/journal.pone.0101219.t003